International Journal of Thermophysics, Vol. 18, No. 1, 1997

Simulation of a Glass Transition in a Hot-Wire Experiment Using Time-Dependent Heat Capacity

O. Andersson[1]

Received May 13, 1996

The transient hot-wire method is used for simultaneous measurements of the thermal conductivity λ and the heat capacity per unit volume ρc_p and yields a peak in λ and a dip in ρc_p near a glass transition. Through simulations, it is shown that these anomalous results arise due to a time dependence in c_p, which is described by a fractional exponential function: $c_p(t) = c_p(\text{liquid}) + [c_p(\text{glass}) - c_p(\text{liquid})]\, e^{-(t/\tau)^{\beta}}$, where τ is the heat capacity relaxation time and β is a sample dependent parameter ($0 < \beta \leq 1$). By a comparison with experimental data for cyclohexanol and glycerol, it is demonstrated that this model can be used to reproduce the peak and the dip as well as the temperature at which these occur. In addition, it is shown that the maximum in λ occurs at $\tau = 0.3$ s, whereas τ of the minimum in ρc_p is dependent on β and moves from 0.4 to 1 s for a change in β from 1 to 0.5. The difference in τ between the peak and the dip is in agreement with the experimental results. It is concluded that the anomalies reveal glass forming characteristics such as a rough classification in terms of strong and fragile glass formers.

KEY WORDS: glass transition; heat capacity; hot-wire method; relaxation; thermal conductivity.

1. INTRODUCTION

If a phase that exhibits molecular diffusion and/or reorientation is cooled rapidly enough to circumvent a phase transition, then a glass state will eventually be produced. The attribute of a glass is positional and/or orientational disorder which is frozen-in on the time scale of observation. This occurs at the glass transition temperature T_g, which separates an equilibrium supercooled state and the nonequilibrium glassy state. In the latter, the molecules cannot move fast enough to establish a new equilibrium state

[1] Department of Experimental Physics, Umea University, 90187 Umea, Sweden.

0195-928X/97/0100-0195$12.50/0

imposed by an external perturbation, e.g., a temperature change. Since a supercooled liquid does not exhibit the lowest Gibbs free energy, equilibrium refers here to a *metastable* state.

One way to probe a glass transition is to measure a property, such as the isobaric heat capacity c_p, as a function of temperature. With increasing temperature, the signature of a glass transition is an abrupt increase in c_p, which reflects the onset of molecular motions, and it is well-known that the increase shifts to higher temperatures with increasing heating rate. Since T_g is taken as the temperature where c_p changes abruptly, it depends on the heating rate or time scale used in the experiment, which in practice can be varied in the range 10^{-2} K · min^{-1} (adiabatic calorimetry) to 10^{2} K · min^{-1} (differential scanning calorimetry).

Another way to study the formation of a glass is through quasi-isothermal relaxation time measurements. The molecular motions become increasingly slow with decreasing temperature, which can be observed in responses to external perturbations. For example, after a step change in the (external) pressure, the sample volume will change with time toward new equilibrium value and the (volume) relaxation time τ can be determined. The result is a measure of τ for the motions on the microscopic level since the time taken to relax will depend on these and, consequently, on T_g. Relaxation can also be studied in the frequency domain using a sinusoidally varying perturbation, e.g., an electric field. At low enough frequencies, τ for diffusional (and/or reorientational) motions is short in comparison with the rate of change in the molecular equilibrium positions, which is imposed by the perturbation As a consequence, the molecules appear mobile in a low-frequency experiment. At high frequencies, this is not the case since the motions are too slow to adjust to the rapid changes of the equilibrium state. Consequently, properties will generally be dependent on the probe frequency ν, especially near $\nu = 1/(2\pi\tau)$, which provides a rough limit between the low- and the high-frequency ranges in which the molecules can or cannot follow the changes of the equilibrium state, respectively. Many properties, such as volume, enthalpy and dielectric permittivity, show observable relaxation associated with a glass transition and often exhibit values for $\tau(T)$ within the same order of magnitude. To present values for T_g from relaxation time measurements, a fairly common practice is to assign it to the temperature where τ is about 10^3 s.

For the purpose of the following discussion, it is useful to correlate the time-scales of the two methods used to study glass transitions: temperature scanning experiments and quasi-isothermal relaxation time experiments. In the latter, it is of course straightforward to state the time scale associated with T_g, e.g., $\tau = 10^3$ s. Unfortunately, there is no general expression which relates this value to a specific cooling and heating rate since the relation

depends on the glass former [1–3]. However, using cooling rates lower than 1 K · min $^{-1}$ should in general yield a T_g which corresponds to $\tau \geqslant 10^3$ and is referred to as (calorimetric) T_g.

In an interesting study of relaxation, Birge [4] investigated the frequency dependence of c_p by electrically heating a thin metal surface in contact with a glass former (glycerol). Using alternating current of a frequency which could be set, the heat wave frequency could be varied in the range 10^{-2} to 10^3 Hz. At isothermal measurements just above T_g, an abrupt step decrease in the measured values for c_p vs frequency was observed. The measurements yield the product of thermal conductivity and heat capacity per unit volume but the step was attributed to the latter. This decrease can be explained in terms of molecular motions not being able to follow a heat wave of high frequency and therefore not contributing to c_p. That is, the motions which become "immobile" at T_g cause the observed decrease in c_p above T_g because of the relatively short experimental time scale (10^2 to 10^{-3} s). Recently, the same effect has been investigated in other glass-forming systems [3, 5]. These results of a frequency dependence in c_p, which is analogous to a time-dependent c_p, are used to explain anomalies in data measured above T_g using the transient hot-wire method. Furthermore, it is shown that these anomalies reveal characteristics of glass formers.

The transient hot-wire method is a fast and convenient method to determine thermal conductivity λ and heat capacity per unit volume ρc_p [6–8]. The principle of the method is that a metal wire (the hot wire) is immersed in a substance for which λ and ρc_p are to be determined (Fig. 1). The wire is electrically heated by a short pulse (1.4 s) and its temperature

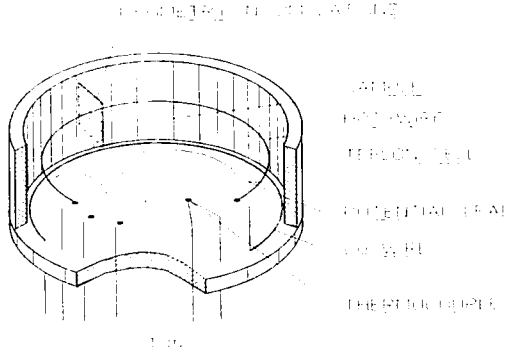

Fig. 1. The sample cell used in hot-wire experiments and the geometry in finite-element analysis of the hot-wire temperature rise.

increase with time t is determined. This is done by measurements of the wire resistance, which depends on the wire temperature T. An exact expression for $T(t)$ of the wire in terms of λ and ρc_p of the substance has been derived for an infinitely long wire [9] and it follows that the desired properties can be obtained by a fitting procedure. It is important to note that the values for λ and ρc_p are assumed to be time independent in the analysis. The advantages of the hot-wire method compared to a steady-state method is that long-time waiting for steady state is avoided and that the shape as well as the exact size of the samples is unimportant in the analysis. However, the samples must be sufficiently large so that heat reflected against the sample cell wall does not interfere with the temperature rise of the hot wire.

The hot-wire method was initially applied to fluids [6] and has later been developed for solids using high pressure to produce good thermal contact between the wire and the solid [7, 8]. This improvement enabled studies of λ and ρc_p of glass formers and it was observed that the method yielded a peak in λ and a dip in ρc_p near T_g of glycerol [10]. The same behavior has thereafter been observed in numerous investigations such as

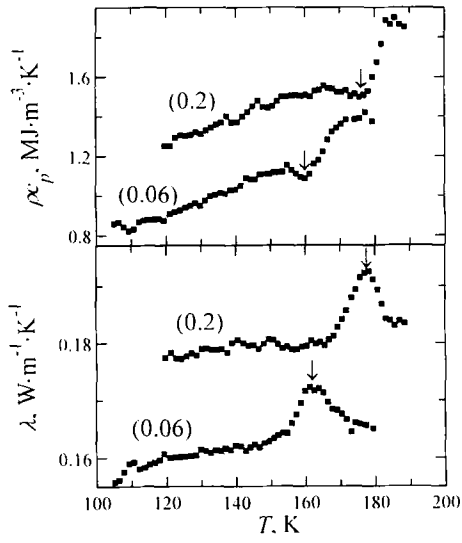

Fig. 2. Experimental results for thermal conductivity and heat capacity per unit volume of cyclohexanol plotted against temperature for pressures in GPa given in parentheses [13]. Arrows indicate peaks and dips which are signatures of a glass transition. (The data for ρc_p at 0.2 GPa have been shifted vertically for clarity.)

those of poly(vinyl acetate) [11], silicone oils [12], and cyclohexanol [13] (Fig. 2). Sandberg et al. [10], suggested that the anomalous values for λ and ρc_p of glycerol were connected to the glass transition relaxation. As described, T_g is associated with the process of some modes of motion becoming immobile on cooling. In a simple model, these modes can be excited almost instantaneously at temperatures well above T_g, whereas below T_g they cannot be excited within the time of an experiment. According to Sandberg et al. [10], the anomalies occur in the temperature range between these two extremes where the modes become possible to excite during the hot-wire pulse of 1.4 s. In other words, the anomalies arise due to changes in c_p during the hot-wire heat pulse, an assumption which is supported by experimental data [3–5]. In this investigation, it is shown that the hypothesis of Sandberg et al. [10] is correct and that the hot-wire anomalies arise due to time dependence in c_p.

2. CALCULATIONS AND RESULTS

2.1. Theory for Hot-Wire Experiments

If an infinitely long hot-wire is heated, then its temperature rise is calculated by solving the heat transfer equation in two dimensions (Fig. 1). In fact, the problem can even be reduced to one dimension because of the radial symmetry. In the approximation of an infinitely long hot wire, the heat transfer equations for the hot wire and the surrounding sample are given by

$$\frac{\partial^2 T}{\partial r^2} + \frac{1}{r}\frac{\partial T}{\partial r} - \frac{1}{a_1}\frac{\partial T}{\partial t} = -\frac{q}{\lambda_1 \pi r_1^2} \tag{1}$$

$$\frac{\partial^2 T}{\partial r^2} + \frac{1}{r}\frac{\partial T}{\partial r} - \frac{1}{a_2}\frac{\partial T}{\partial t} = 0 \tag{2}$$

where r is the radial coordinate, a ($=\lambda/\rho c_p$) is the thermal diffusivity, and q is the power supplied per unit length of the hot wire. The subscripts 1 and 2 refer to the hot wire and sample, respectively. The exact solution of Eqs. (1) and (2) for the temperature rise ΔT of the hot wire of radius r_1 in an infinitely large sample is [9]

$$\Delta T = \frac{2q\alpha^2}{\pi^3 \lambda_2} \int_0^\infty \frac{1 - e^{(-a_2 u^2 t)}}{u^3 \Delta(u, \alpha)}\, du \tag{3}$$

where

$$\Delta(u, \alpha) = [uJ_0(u) - \alpha J_1(u)]^2 + [uY_0(u) - \alpha Y_1(u)]^2$$

$$\alpha = 2\rho_2 c_{p2}/\rho_1 c_{p1}$$

J_0 and J_1 are Bessel functions of the first kind of zeroth and first order and Y_0 and Y_1 are Bessel functions of the second kind of zeroth and first order.

2.2. Glass Transition Model

In hot-wire experiments, values for ΔT versus t are measured and Eq. (3) is fitted to these, yielding λ and ρc_p of the sample. However, in this case, we use Eqs. (1) and (2) to calculate theoretical values for ΔT versus t which would be obtained at a glass transition and, subsequently, fit Eq. (3) to these simulated data. In order to this, we must introduce the effect of relaxation on the data for ΔT versus t. This is accomplished by assigning the heat capacity of the sample c_{p2} a time dependence. In the model, $c_{p2}(t \to 0)$ is given by the heat capacity of the glass $c_{p2}(\text{glass})$. This is based on the assumption that only the modes which normally can be excited in the glassy state can respond quickly enough to absorb heat and, consequently, contribute to c_p. If the measurement time approaches infinity, however, then c_{p2} will be equal to the heat capacity of the liquid c_{p2} (liquid), which is observed above T_g. The rate at which c_p of the sample changes between these two limiting values depends on the temperature and is conveniently described in terms of the relaxation time $\tau(T)$. With increasing temperature, $\tau \to 0$ since the molecules respond quicker to a perturbation, and consequently, $\tau \to \infty$ with decreasing temperature. In this case, we assume that a fractional exponential function provides a good description for $c_{p2}(t)$ in terms of the relaxation time. This assumption yields

$$c_{p2}(t) = c_{p2}(\text{liquid}) + [c_{p2}(\text{glass}) - c_{p2}(\text{liquid})]e^{-(t/\tau)^{\beta}} \tag{4}$$

where β has a value between 0 and 1. The fractional exponential function has been successful in describing various relaxation data and was also favorably employed by Birge [4]. It should be emphasized that c_p of the glass and the liquid states provide values for the initial and infinite times, respectively, and that the sample is *not* regarded as consisting of glassy and liquid domains. In a first attempt to reproduce the hot-wire results, we use $\beta = 1$ (simple exponential) and the values for c_p of the glassy and liquid states are taken from experimental results.

2.3. Results and Comparison with Experiments for Cyclohexanol

Equations (1) and (2) can be solved numerically using finite-element analysis [14] and the temperature of the hot wire can be calculated as a function of time. The following data, which are typical for a hot-wire experiment, were used: $r_1 = 5 \times 10^{-5}$ m, $q = 0.95$ W · m^{-1}, $\lambda_1 = 70$ W · m^{-1} · K^{-1}, and $\rho_1 c_{p1} = 2 \times 10^6$ J · m^{-3} · K^{-1}. In our case, we compare the results from the calculations with the experimental results for cyclohexanol [13] (Fig. 2) and glycerol [15]. The source phase of the glassy state of cyclohexanol discussed here is a plastic crystalline phase [13] but the discussion is valid also for liquid glass formers such as glycerol. To keep the terminology simple and more familiar, it is therefore referred to as a liquid. If Eq. (4) is multiplied by density, then we can insert $\rho_2 c_{p2}(\text{liquid}) = 1.39 \times 10^6$ J · m^{-3} · K^{-1} and $\rho_2 c_{p2}(\text{glass}) = 1.13 \times 10^6$ J · m^{-3} · K^{-1}, which are obtained from the experimental results at 0.06 GPa (Fig. 2). In addition, we extract $\lambda_2 = 0.163$ W · m^{-1} · K^{-1} just below and above the peak in λ. Above the peak, λ is slightly larger but the difference is small and can, in this case, be attributed to the crystallization, which occurs above T_g and is clearly observed just outside the range shown here. All parameters needed to calculate the temperature rise of the hot wire are now available and the results are shown in Fig. 3 for the relaxation times of 0.01 and 10 s ($\beta = 1$).

After calculation of $\Delta T(t)$ for a selected set of relaxation times, Eq. (3) was fitted to these data using λ_2 and $\rho_2 c_{p2}$ as fitting parameters (solid lines in Fig. 3). All other data were the same as those used in the initial calculations. Consequently, results associated with relaxation times well above $T_g(\tau \to 0)$ should yield $\lambda_2 = 0.163$ W · m^{-1} · K^{-1} and $\rho_2 c_{p2} = 1.39 \times 10^6$ J · m^{-3} · K^{-1}

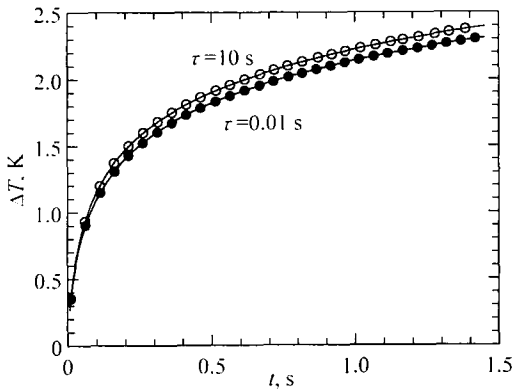

Fig. 3. Calculated results for temperature rise of the hot wire plotted against time for two relaxation times. The solid lines are fits given by Eq. (3).

(liquid), whereas results below $T_g(\tau \to \infty)$ should yield $\lambda_2 = 0.163$ W · m^{-1} · K^{-1} and $\rho_2 c_{p2} = 1.13 \times 10^6$ J · m^{-3} · K^{-1} (glass). As shown in Fig. 4, this is indeed the case. The interesting range is between these limits where a peak and a dip apparently occur in λ and ρc_p, respectively, exactly as noticed in experiments. Moreover, we find that the maximum in λ occurs at $\tau \approx 0.3$ s, whereas the minimum in ρc_p appears at $\tau \approx 0.4$ s. As discussed below, this difference in τ is consistent with experimental results.

Since the model reproduces the anomalous experimental results observed at many glass transitions well, it is possible to explore the extent to which various parameters affect the peak and dip shapes. The result can be used for characterization of glass formers and also explain why some of these, such as C_{60} [16], do not exhibit anomalies. Initially, we investigate the effect of a change in the relaxation function. The calculations described above were repeated using a fractional exponential function with $\beta = 0.5$ instead of the simple exponential relaxation function [$\beta = 1$ in Eq. (4)]. As shown in Fig. 4, a smaller value for β gives a smaller but broader peak and dip. This is consistent with an interpretation of β as a measure of the relaxation time distribution. That is, the sample response to a perturbation cannot be described by a single independent

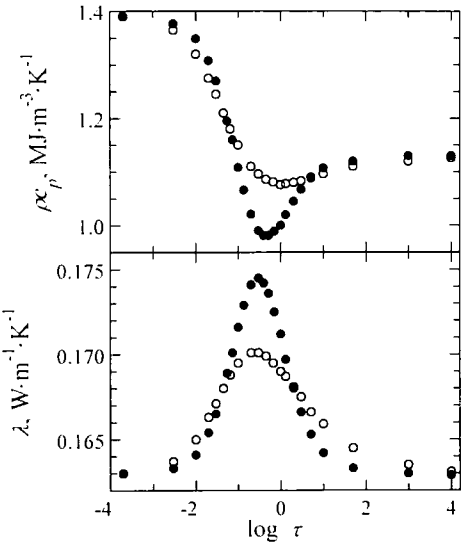

Fig. 4. Calculated results for thermal conductivity and heat capacity per unit volume of cyclohexanol plotted against logarithm of relaxation time (in seconds) for two relaxation functions: (●) $\beta = 1$; (○) $\beta = 0.5$ [see Eq. (4)].

relaxation process and therefore not by a single τ at each temperature. The smaller the value for β, the larger the distribution of relaxation times and, as a consequence, the broader the distribution of the relaxation effect (broader peak and dip). In addition to this result, the calculations for $\beta = 0.5$ show that the maximum in λ still occurs at $\tau = 0.3$ s but the minimum in ρc_p moves to $\tau = 1$ s.

Since the time dependence in c_p becomes less pronounced as the step in c_p at T_g decreases, it is obvious that the sizes of the anomalies should also depend on the size of the step. To quantify this, the step in c_p was reduced to half of that used in the calculations above ($\beta = 1$). The peak size $[= \lambda_{max} - \lambda(\tau \to 0)]$ decreased to 0.06 from 0.12 $W \cdot m^{-1} \cdot K^{-1}$ for the full step in c_p, which indicates that it is proportional to the step size in c_p. It follows that glass formers which exhibit large differences in c_p between the glassy and the liquid states are more likely to exhibit anomalous results in λ and ρc_p near T_g. Furthermore, the result can be used to understand the smaller and broader peak when there is a distribution of relaxation times. Instead of using a smaller value for β to account for a distribution, one can divide the total step in c_p at T_g in several smaller steps, each of which is associated with the excitation of a specific mode and described by a simple relaxation function. In other words, we imagine that the glass transition consists of several subtransitions which occur in a narrow temperature range. In order just to show the effect of such a division, we use the simplest distribution of only two simple relaxation functions and assume that these are associated with the relaxation times τ_1 and $2\tau_1$. That is, increasing the temperature from below to well above T_g will add two modes of motions, and the τ of one of these is twice as large as that of the other (at all temperatures). Moreover, we assume that each mode accounts for half of the total step in c_p. Based on the calculations above, it would result in two equally sized peaks in $\lambda(\tau_1)$, of a magnitude half of that corresponding to one simple relaxation function, and maxima at $\tau_1 = 0.3$ and 0.15 s, respectively. It follows that a continuous distribution of relaxation times results in a smaller but broader peak. We can conclude that for a given step in c_p at T_g, glass formers which are described by a simple exponential relaxation function should show the most pronounced anomalies in λ and ρc_p.

In order to compare directly the theoretical results with the experimental data, the relaxation times must be related to temperatures. To do this, we can assume that literature data for $\tau(T)$ [17] determined from both dielectric relaxation ($\tau < 10^3$ s) and enthalpy relaxation ($\tau > 10^3$ s) at atmospheric pressure provide a good description. The temperatures for the simulated data shown in Fig. 5 were calculated using these results. Since the experiments were performed at elevated pressure, and T_g increases

slightly with pressure, the measured data were recalculated from 0.06 GPa to atmospheric pressure by a temperature shift of -6 K (the results in Fig. 2 yield $\Delta T_{peak}/dP \approx 100$ K · GPa $^{-1}$). The temperatures for the maxima in λ differ only by 2.5 K between the experiment and the simulations, which is about the same as the inaccuracies in these results. The inaccuracy in the temperature determination in hot-wire experiments is ± 0.5 K and the recalculation to atmospheric pressure causes an additional uncertainty of ± 0.5 K. Another possibility for the difference is disagreement between dielectric[17] and heat capacity relaxation times, and a factor of 2 would be sufficient to account for the small temperature difference observed here. In addition to this result, the widths as well as the sizes of the peaks and dips are of the correct magnitude. The peak size in the experiment is between that for $\beta = 1$ and that for $\beta = 0.5$, indicating that the heat capacity relaxation of cyclohexanol is best described with $0.5 < \beta < 1$ (no value for β of cyclohexanol could be found in the literature). The exact experimental value for the maximum in λ could be reproduced using $\beta \cong 0.8$. Dielectric relaxation data of the similar glass former cyclooctanol can be described with $\beta \cong 0.7$ [18], indicating that the value is realistic.

In a detailed analysis of the experimental data, it can be seen that the maximum in λ occurs at about 2.5 K higher temperature than does the

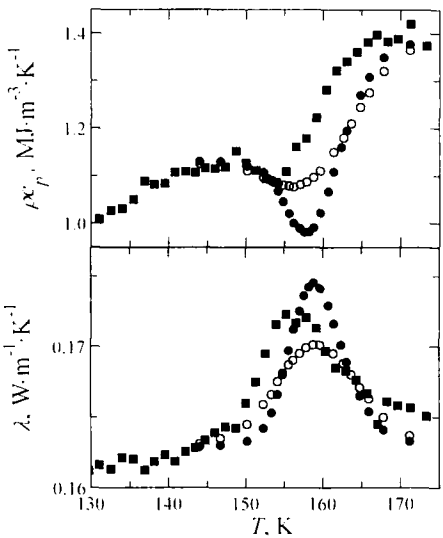

Fig. 5. Thermal conductivity and heat capacity per unit volume of cyclohexanol plotted against temperature. (■) Experimental results recalculated to atmospheric pressure (see text). Simulations: (●) $\beta = 1$; ( ) $\beta = 0.5$.

minimum in ρc_p. This difference can be compared with 0.5 K ($\beta = 1$) and 2.5 K ($\beta = 0.5$) obtained in the simulations. Consequently, the simulations reproduce a difference in temperature of correct size.

The peak and the dip have occasionally been used to provide data for T_g and, apparently, correspond to $\tau \approx 0.3$ s. Since we know $\tau(T)$ for cyclohexanol, it is possible to estimate the difference in temperature between this result and that from the more commonly employed assignment $\tau(T_g) = 10^3$ s, which corresponds better to the calorimetric T_g. This yields a difference of about 12 K. In addition, we can obtain a general result for this difference which is based on a classification of glass formers. In this classification, glass formers for which τ vary rapidly with temperature near T_g are referred to as "fragile," whereas a weak dependence is a signature of a "strong" glass former [19, 20]. For the latter $\partial(\log \tau)/T_g \partial(1/T)$ is about 17, whereas that for a fragile glass former can be at least 90 near T_g [19], assuming that τ is proportional to the viscosity. The differences in temperature between the peak in λ and $T_g(\tau = 10^3 \text{ s})$ are then roughly given by $0.21T_g$ and $0.04T_g$ for strong and fragile glass formers, respectively. It follows that the temperature difference between the hot-wire anomalies and the calorimetric T_g provides a rough strong–fragile classification of the glass former. Another way to compare strong–fragile glass formers is to plot $\log \tau$ vs T/T_g [19, 20], which roughly can be obtained in the relaxation time range where the anomalies are observable (10^{-2}–10^2 s).

2.4. Results and Comparison with Experiments for Glycerol

The calculations described above were repeated for glycerol. In this case, however, the temperature dependence of ρc_p for both the glass and the liquid states was accounted for in the calculation of the hot-wire temperature rise. Two linear functions of temperature were fitted to experimental data for ρc_p of glycerol (Fig. 6), yielding $\rho c_p(\text{glass}) = 4890T + 4.02 \times 10^5$ and $\rho c_p(\text{liquid}) = 9480T + 5.91 \times 10^5$. The value for λ was approximated by a constant value of 0.355 $\text{W} \cdot \text{m}^{-1} \cdot \text{K}^{-1}$, which is a good approximation for temperatures below the peak in λ but a slight overestimation above the peak (Fig. 6). Moreover, a literature value for $\beta = 0.65$ [Eq. (4)] of glycerol was used together with results for the temperature dependence of $\tau = [2\pi 10^{14.6} \exp(-2500/(T - 128))]^{-1}$ [4]. The experimental data for λ and ρc_p were recalculated from the measurement pressure of 0.16 GPa to atmospheric pressure by a temperature shift of 7 K, which follows from the result $(dT_g/dP)_{0.08\text{GPa}} = 44 \text{ K} \cdot \text{GPa}^{-1}$ [10].

As shown in Fig. 6, the sizes of the anomalies are in good agreement, whereas the widths are slightly larger for the calculated results. However, the experimental difference in λ ($\approx 5\%$) between results above and below

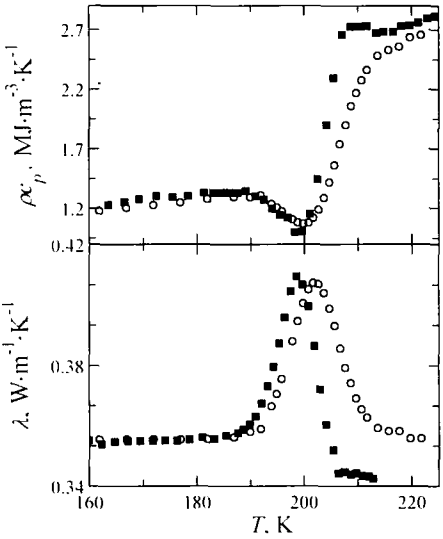

Fig. 6. Thermal conductivity and heat capacity per unit volume of glycerol plotted against temperature. (■) Experimental results [15] recalculated to atmospheric pressure (see text). Simulations: ( ) $\beta = 0.65$.

the peak (Fig. 6) indicates that λ should also be slightly time dependent, which must be accounted for to obtain perfect agreement.

A detailed analysis of the maxima in λ and minima in ρc_p shows that experimental anomalies occur at temperatures which are about 1 K apart, whereas the calculated results give a difference of 2 K. That is, in this case the calculation overestimates this difference, which was slightly underestimated in the case of cyclohexanol. Moreover, the calculated anomalies are shifted about 3 K to higher temperatures than those of experimental anomalies, which is of the order of the inaccuracy. The peak temperature is about 200 K, which is 17 K higher than T_g ($= 183$ K) for glycerol [21]. This result ($T_{peak} - T_g = 0.1 T_g$) yields a classification of glycerol as an intermediate glass former, which is in agreement with a detailed analysis [19].

3. DISCUSSION AND SUMMARY

The key feature of this work is that c_p exhibits a time dependence near T_g which can affect the results from measurements utilizing a transient method. In particular, anomalous experimental data for λ and ρc_p of a

hot-wire experiment are described very well by such a model. In the normal analysis of hot-wire data, it is assumed that c_p is constant during the 1.4 s of a measurement. If c_p increases during this time, then the assumption leads to a peak in the values for $\lambda(T)$ and a dip in those for $\rho c_p(T)$. These anomalies are good signatures of a glass transition and therefore provide useful information. Furthermore, their positions in temperature as well as their widths and sizes reveal characteristics of the glass former. In particular, the simulations show that the shapes of the anomalies depend on the following.

(a) The relaxation function. In terms of the fractional exponential function, the features in λ and ρc_p are more pronounced the larger the value for β and, consequently, largest for a glass former that exhibits a simple exponential relaxation function ($\beta = 1$). That is, the widths decrease and the sizes increase with increasing β.

(b) The difference in c_p between the glassy state and its source phase. The larger the step in c_p, the larger sizes for the anomalies.

(c) The relation between relaxation time and temperature. This has not been shown explicitly but it is obvious that this relation affects the peak and dip shapes. The stronger τ depends on temperature for values of τ in the range 10^{-2}–10^{2} s (see Fig. 4), the more pronounced anomalies because of decreasing widths. Consequently, a fragile glass former should exhibit more pronounced anomalies than strong ones since their $\tau(T)$ increase abruptly near T_g.

The best conditions for observing large anomalies may not all be fulfilled by one glass former. A simple exponential relaxation function is normally not observed for fragile glass formers near T_g [19]. Consequently, the best conditions of (a) and (c) are in general not found for the same glass former. On the other hand, fragile glass formers, in comparison with strong glass formers, commonly exhibit a large step in c_p at T_g [19]. Hence, the best condition of (b) generally follows from that of (c). Taking all these considerations into account, fragile glass formers probably exhibit the best systems for observing glass transition anomalies in hot-wire experiments. For strong glass formers, such as C_{60} and SiO_2, which show very small steps in c_p at T_g, the anomalies might be impossible to detect. (For C_{60} it is, however, possible to observe a discontinuity in $d\lambda/dT$ at T_g [16].

The results here of time-dependent c_p substantiate previous results from measurements of frequency dependence in c_p [3–5]. The abrupt decrease in c_p versus frequency observed by Birge [4] is of the same

magnitude as the c_p step at T_g in a measurement using differential scanning calorimetry, which is in quantitative agreement with the result found here in the time domain. This result verifies that the frequency dependence in c_p is associated with the modes which become "immobile" below T_g in temperature scanning experiments. If these modes are probed on a sufficiently short time scale, then they cannot follow the heat wave and therefore do not contribute to c_p even in a supercooled liquid state.

In summary, the hot-wire method can be used to probe time dependence in c_p, yielding characteristics of glass formers. A peak in λ and a dip in ρc_p are signatures of a relaxation associated with a glass transition. Their positions in temperature and their shapes provide a rough strong–fragile classification as well as a description of the relaxation function.

ACKNOWLEDGMENTS

The author thanks Dr. Per Jacobsson and Dr. Hans Forsman for useful discussions. This work was supported by the Swedish Natural Research Council.

REFERENCES

1. W. Götze and L. Sjögren, *Rep. Prog. Phys.* **55**:241 (1992).
2. E. Donth, *J. Non-Cryst. Solids* **53**:325 (1982).
3. A. Hensel, J. Dobbertin, J. E. K. Schawe, A. Boller, and C. Schick, *J. Thermal. Anal.* **46**:935 (1996).
4. N. O. Birge, *Phys. Rev. B* **34**:1631 (1986).
5. Y. H. Jeong and I. K. Moon, *Phys. Rev. B* **52**:6381 (1995).
6. J. J. Healy, J. J. de Groot, and J. Kestin, *Physica* **82C**:392 (1976).
7. P. Andersson and G. Bäckström, *Rev. Sci. Instrum.* **47**:205 (1976).
8. B. Hakansson, P. Andersson, and G. Bäckström, *Rev. Sci. Instrum.* **59**:2269 (1988).
9. H. S. Carslaw and J. C. Jaeger, *Conduction of Heat in Solids*, 2nd ed. (Clarendon Press, Oxford, 1959), pp. 341–344.
10. O. Sandberg, P. Andersson, and G. Bäckström, in *Proc. 7th Symp. Thermophys. Prop.*, A. Cezairliyan, ed. (ASME, New York, 1977), pp. 181–184.
11. O. Sandberg and G. Bäckström, *J. Polym. Sci.* **18**:2123 (1980).
12. O. Sandberg and B. Sundqvist, *J. Appl. Phys.* **53**:8751 (1982).
13. O. Andersson, R. G. Ross, and G. Bäckström, *Mol. Phys.* **66**:619 (1989).
14. G. Bäckström, *Fields of Physics on the PC by Finite Element Analysis* (Studentlitteratur, Lund, 1994).
15. O. Andersson, Ph.D. thesis (Umea University, Umea, 1991).
16. O. Andersson, A. Soldatov, and B. Sundqvist, *Phys. Lett. A* **206**:260 (1995).
17. K. Adachi, H. Suga, S. Seki, S. Kubota, S. Yamaguchi, O. Yano, and Y. Wada, *Mol. Cryst. Liq. Cryst.* **18**:345 (1972).
18. D. L. Leslie-Pelecky and N. O. Birge, *Phys. Rev. Lett.* **72**:1232 (1994).
19. C. A. Angell, *J. Non-Cryst. Solids* **131–133**:13 (1991).
20. S. R. Elliott, *Physics of Amorphous Materials*, 2nd ed. (Longman Group UK Ltd., Hong Kong, 1990).
21. B. Wunderlich, *J. Phys. Chem.* **64**:1052 (1960).